Nanostructuring Lipophilic Dyes in Water Using Stable Vesicles – Quatsomes – as Scaffolds and their use as Probes for Bioimaging

Antonio Ardizzone, Siarhei Kurhuzenkau, Sílvia Illa-Tuset, Jordi Faraudo, Mykhailo Bondar, David Hagan, Eric Van Stryland, Anna Painelli, Cristina Sissa, Natalia Feiner, Lorenzo Albertazzi, Jaume Veciana, Nora Ventosa**

Dr. A. Ardizzone, Dr. J. Faraudo, Dr. N. Ventosa, Prof. J. Veciana
Institut Ciencia Materials Barcelona (CSIC)-CIBER-BBN, Campus Universitari de Bellaterra, 08193-Cerdanyola, Spain
E-mail: ventosa@icmab.es, veciana@icmab.es
S. Illa-Tuset
Theoretical Sciences Unit, JNCASR,
Bangalore 560064, India
Prof. M. Bondar
Institute of Physics, National Academy of Sciences of Ukraine, Prospect Nauky 46, Kyiv, Kyiv-03028, Ukraine
Dr. D.J. Hagan, Prof. E.W. Van Stryland
The College of Optics and Photonics (CREOL), University of Central Florida, P.O. Box 162700, Orlando, FL, USA
Prof. A. Painelli, Dr. C. Sissa, Dr. S. Kurhuzenkau
Università di Parma, Parco Area delle scienze 17/A
43124 Parma, Italy
N. Feiner, Dr. L. Albertazzi
Institute for Bioengineering of Catalonia (IBEC), Parc Cientìfic de Barcelona (PCB), 08028 Barcelona, Spain

Keywords: vesicles, dyes, fluorescent nanoparticles, Molecular Dynamics, STORM

Abstract: A new kind of fluorescent organic nanoparticles (FONs) is obtained using Quatsomes (QS), a family of nanovesicles proposed as scaffolds for the nanostructuration of commercial lipophilic carbocyanines (DiI, DiD and DiR) in aqueous media. The obtained FONs, prepared by a CO_2-based technology, show excellent colloidal- and photo-stability, outperforming other nanoformulations of the dyes, and improve the optical properties of the fluorophores in water. Molecular dynamics (MD) simulations provide an atomistic picture of the disposition of the dyes within the membrane. The potential of QS for biological imaging has been demonstrated performing super resolution microscopy of the DiI-loaded vesicles *in*

vitro and in cells. Therefore, fluorescent Quatsomes constitute an appealing nanomaterial for bioimaging applications.

Fluorescent organic dyes are widely investigated as fluorescent probes in microscopy, thanks to their tunable optical and physicochemical properties via chemical modification of their structure.[1] Good fluorescent probes for microscopy should be bright and highly photostable, water-soluble and chemically stable in buffers, cell media or body fluids, as well as capable of site-specific labeling and showing biocompatibility.[2] Small organic molecules can be highly fluorescent, although they may suffer poor solubility in aqueous media (particularly so for red and infrared dyes),[3] limiting their use for bio-applications.[4] Loading an organic dye into a non-fluorescent nanocarrier, arranged as fluorescent organic nanoparticle (FON), offers an interesting strategy to bring organic dyes in aqueous media, since the obtained FONs have in general good brightness, photostability and biocompatibility.[5–9] These nanostructures also have well-known physico-chemical properties and can be loaded or grafted with bioactive compounds and/or targeting agents, to produce multi-functional nanoparticles for theranostic applications.[10]

Small unilamellar vesicles (SUVs), e.g. liposomes, with sizes ~100 nm, are intensively investigated supramolecular nanostructures for such purposes.[11,12] Indeed, their membranes offer opportunities for an efficient functionalization and for this reason they find various biological applications, including drug delivery, labeling and bioimaging.[11,13,14] In spite of extensive studies on SUVs, only a few works have been focused on their capability to nanostructure organic dyes.[15–17] Moreover, there is a strong interest towards new vesicular formulations, made by non-lipid components, able to overcome the intrinsic instability of liposomes that hinders their biomedical applications.[18]

Here we present Quatsomes (QSs), a new class of exceptionally stable SUVs with sizes smaller than 100 nm, formed by the self-assembly in water of CTAB and cholesterol in a 1:1 ratio, as effective colloidal nanostructures for loading lipophilic and water insoluble organic dyes resulting in highly stable and bright FONs.[19] Dye-loaded QSs can be prepared by a one-step method using compressed CO_2, named Depressurization of Expanded Liquid Organic Solution-Suspension (DELOS-SUSP), showing several advantages over conventional routes for the preparation of functionalized vesicles. Indeed, it is a green technology leading in a single step to the formation of multifunctional nanovesicles with superior structural homogeneity.[20–22]. As dye models, we used lipophilic fluorophores with long alkyl chains, which can be integrated into QSs membrane exploiting hydrophobic interactions between the chains of the dyes and the hydrophobic compartment of the double-layer membrane. Specifically, we use three water-insoluble carbocyanine dyes with two 18-carbons aliphatic chains, 1,1'-dioctadecyl-3,3,3',3'-tetramethyl-indocarbocyanine perchlorate (DiI), 1,1'-dioctadecyl-3,3,3',3'-tetramethyl-indodicarbocyanine perchlorate (DiD) and 1,1'-Dioctadecyl-3,3,3',3'-tetramethylindotricarbocyanine iodide (DiR) (**Figure 1**).[23,24] Our experimental results are supported by Molecular Dynamics simulations (MD) which gave information on the configuration of the dyes within the membrane and we finally explore the potential of the dye-loaded Quatsomes for biological imaging using dye-loaded QSs as probes for Stochastic Optical Reconstruction Microsopy (STORM), an innovative super-resolution microscopy technique.[25]

DiD-loaded Quatsomes with DID loadings, L = $moles_{DID}/(moles_{CTAB}+moles_{Cholesterol})$, ranging from 0.6 x 10^{-3} to 6,6 x 10^{-3} (**Table S1**) were prepared using the DELOS-SUSP methodology.[21] The physico-chemical properties of the resulting vesicles with L = 1.3 x 10^{-3} (D-QS-2) are here compared with those of other DiD-loaded Quatsomes obtained by other methods generally used for the preparation of loaded vesicles, such as incubation (D-QS-2-IC),[26] sonication (D-QS-2-SON)[19] and thin film hydration (D-QS-2-TFH).[27] The

normalized UV-Vis absorption spectra of DiD-loaded QSs prepared by different routes are shown in **Figure 1** for comparison along with the spectra of solvated DiD in ethanol (EtOH) and nanoparticles of pure DiD (D-NP) in water, obtained by DELOS-SUSP method but without using the surfactant (see SI). Absorption spectra of DiD-loaded QSs obtained by DELOS-SUSP (D-QS-2) and by thin film hydration (D-QS-2-THF) are very similar to the spectra of solvated DiD in EtOH, showing a narrow band with well-resolved vibronic structure. All other samples show broad spectra with the appearance of intense features on the blue wing of the band, pointing to the formation of H-aggregates,[23,24,28] in line with the well-known tendency of cyanines to aggregate.[28–30] The similarity of spectra of DiD-loaded QSs prepared by DELOS-SUSP and TFH methods suggest that the dye molecules are well dispersed as isolated species inside the QS membrane. However, as shown in CryoTEM images (**Figure S2**), D-QS-2 vesicles are much more homogenous in terms of size and lamellarity than D-QS-2-TFH. DiD-loaded Quatsomes showed several advantages over other DiD-based FONs, such as D-NP and DiD-loaded CTAB micelles (D-MIC), in terms of both optical and colloidal properties. DiD-loaded QSs are colloidally stable during months, with no appreciable changes in size distributions (**Table S1**) neither in absorption/emission spectra over a two-month period (**Figure 2A**). On the other hand, the absorption of D-NP decreases steadily following the aggregation of the nanoparticles (**Figure S3**). **Figure 2B** compares visible absorption and emission spectra of D-QS-2 and D-NP. The luminescence of D-NP is completely quenched, in line with the formation of H-aggregates, while the fluorescence spectrum of D-QS-2 is very similar in shape to that of solvated DiD in EtOH. The stability upon dilution of D-QS-2 and D-MIC is compared in **Figure S4**. D-QS-2 maintains its fluorescence at different dilutions; while fluorescence of D-MIC is lower at the same dye concentration and it is quenched at concentrations below the critical micellar concentration (CMC) of CTAB, suggesting the rupture of micelles and the formation of non-fluorescent DiD aggregates in water.

The effect of dye-loading on the physico-chemical properties of DiD-loaded QSs was also studied by comparing five different samples with increasing fluorophore loadings with L = 0.6 x 10^{-3} to 6.6 x 10^{-3} prepared by DELOS-SUSP. Samples are listed in **Table S2** along with mean size values, measured by Nanoparticle Tracking Analysis (NTA). Mean diameters and CryoTEM images (**Figure S5**) show that L does not affect the vesicle size and morphology. Corresponding absorption spectra in **Figure S6A** show an increase of the intensity on the blue wing of the absorption band, suggesting the progressive formation of non-luminescent H-aggregates in the QS membrane upon increasing the dye concentration; as confirmed by excitation spectra (**Figure S6B)** whose shape does not change with the dye-loading. The progressive formation of H-aggregates in DiD-loaded QSs with increasing dye loading also explains the decrease of the extinction coefficient (ε) (by a factor ~1.8) and of the fluorescence quantum yield (FQY, from 23% to 7%) (**Table S2**). The marginal loss of FQY in going from solvated DiD in EtOH (31%) to D-QS-1 (23%) can be ascribed either to the formation of a very small amount of aggregates and/or to environmental effects. [24]

DiI- and DiR-loaded Quatsomes (I-QS and R-QS, respectively in **Table S1**) were also prepared by DELOS method with different loadings to study how the length of the conjugated bridge of carbocyanines, *n*, affect the dye aggregation inside the bilayer. Much as for DiD-loaded QSs, the increments in absorbance in the blue wing of R-QS samples points at the formation of H-aggregates (**Figure S7B**). On the opposite, the absorption and excitation spectra of I-QS do not support the formation of DiI aggregates in the membrane (**Figure S7A**). Overall, the length of the conjugated chain (*n*) of carbocyanines strongly affects the brightness (ε x FQY) of fluorescent QSs (**Figure 2C**). In the case of the shortest chain (DiI), nanostructuration over QSs results in higher brightness compared to the dye in EtOH (up to 50% higher), and high values are maintained even at the highest explored loading (**Table S3**). On the contrary, when loaded with DiD and DiR the formation of non-fluorescent aggregates determines a rapid decrease of the FONs brightness. Thus, cyanines with longer conjugated

structures experience stronger π-π interactions upon nanostructuration, as observed in previous works where cyanines with different polymethine chain sizes were intercalated into DNA strands. [31]

Photostability of DiD in EtOH and of DiD-loaded QSs in water was analyzed by monitoring the evolution over time of the absorbance under continuous laser irradiation (**Figure S9**). Relevant photodecomposition quantum yields, determined according to Belfield' method, [32]were obtained (see **Table S2**). DiD-loaded QSs at any of the assayed loadings are more photostable (~2 order of magnitude) than micelle-based nanoformulation of the same dye in water, [33] likely due to the lower photostability of dyes aggregates[34,35] which are more numerous in the micelles than in QSs. However, DiD-loaded QSs were found less photostable compared to the solvated DiD in EtOH and to its hydrophilic analogue Cy5 dissolved in water.

Two-photon absorption spectra of DiD in EtOH, and of D-QS-3 and D-QS-5 in water are shown in **Figure 2D**. Two-photon absorption (2PA) bandshapes are in agreement with previous works in literature on cyanine dyes.[36] Indeed, DiD in EtOH and DiD-loaded QSs in water show a really narrow main 2PA band, as generally known for cyanines, with values of 2PA cross-section around 900 GM. Interestingly, no variations of 2PA bandshapes neither of cross sections were found upon increasing the loading of DiD in QSs or changing the solvent, confirming that there is no major effect of solvent polarity neither on the aggregation state of the dye on 2PA cross-section when DiD is loaded into QSs.

We have employed the NAMD software to perform large-scale Molecular Dynamics (MD) simulations of DiI- and DiD-loaded QSs in water in order to obtain an atomistic picture of the incorporation of these dyes in QS.[37] Due to the large number of atoms involved in the simulations (10^4-10^5) and the long time scales required (>200 ns), we considered only a QS patch with a single dye molecule (DiI or DiD) in water (all technical details of the MD simulations are summarized in the SI). In **Figure 3**, we show snapshots from the simulations and the average atomic density profiles. Both DiD and DiI have their carbocyanine groups in

contact with water, with their nitrogen atoms located in the hydrophilic region of the QS bilayer (i.e., inside the QS region delimited by the headgroups of the CTAB surfactants and the –OH groups of the cholesterol). The carbocyanine groups are on average parallel to the interface for DiD and almost parallel with a small angle of ~2º for DiI. During the simulations we found configurations with one of the two quinoline groups of each carbocyanine located closer to the membrane interior than the other one (which is closer to water). The aliphatic chains in both carbocyanines are immersed inside the hydrophobic layer of the QS, as expected. As seen in **Figure 3**, the presence of a dye affects the two leaflets of the QS bilayer. The distance between the density peaks corresponding to carbocyanine nitrogen atoms and the terminal carbon atom of the aliphatic chains is about ~1.8 nm, compared with the ~3.4 nm size of the hydrophobic layer of the QS. For both dyes we observe a substantial mobility in the QSs with a motion that can be described as a two dimensional Brownian motion (see SI for details), as corresponds to ordinary lateral diffusion over the membrane. We estimate a diffusion coefficient of $D=4\times10^{-11}$ m^2/s for either dye, of a similar magnitude to that of phospholipid molecules in a lipid bilayer.[38]

Having extensively characterized the promising fluorescent properties of cyanines-loaded QSs we then explored their potential for imaging. In particular, we demonstrated that thanks to their colloidal and photochemical stability and to the photophysical properties of the loaded dyes QSs can be used as probes for STORM super resolution microscopy. STORM is an emerging super resolution technique for biology[25] and nanobiotechnology[39,40] allowing multicolor imaging *in vitro* or in cells with nanometric resolution.

Figure 4A shows *in vitro* STORM imaging of DiI-loaded Quatsomes (I-QS-1 sample). DiI photophysical properties inside Quatsomes are suitable for STORM, i.e. they display bright single molecule blinking upon irradiation, allowing accurate molecule localization and reconstruction of super resolved images (**Fig. 4A**, right). DiI distribution appears to be homogenous inside spherical vesicles with subdiffraction size, in agreement with TEM

imaging and spectroscopic characterization (shown in **Figure S7A and S8**). The images have been quantified to extrapolate the average number of dye localizations and the size of the labeled Quatsomes (**Figure 4B**). STORM quantification showed an average size of Quatsomes around 99 nm with a relatively narrow distribution (very few QSs are larger than 200 nm) in agreement with Cryo-TEM results. The localization histogram shows that a large number of DiI molecules is incorporated in the vesicles (mean value of 193 molecular localizations per QS), demonstrating the ability of our formulation to nanostructure a controlled number of dyes into a small vesicle size. The direct visualization and the determination of the exact position in a living biological environment are key aspects of imaging and theranostic agents. For this purpose, DiI-loaded Quatsomes (I-QS-1, diluted at 20 μM CTAB concentration) have been incubated with HeLa cells and live cells intracellular trafficking has been monitored for 1.5 hours using fluorescence microscopy. **Figure 4C** shows a snapshot of the video (see SI) after one hour of incubation. QSs are initially bound to the cellular membrane and subsequently trafficked into cell. After QSs administration, cells were fixed and the internalized vesicles were visualized by STORM, as shown in **Figure 4D.** The size of the individually resolved QSs indicates that the vesicles did not undergo aggregation after internalization in cells in agreement with the *in vitro* studies. Moreover, these measurements show that QS are still assembled inside cells indicating that their high colloidal stability allows for cellular imaging applications. These measurements show that the size, colloidal stability and photophysical properties of dye-loaded QSs make them remarkable candidates as nanostructured probes for biological imaging. These results together with the capability of QSs to integrate/encapsulate small drugs or large biomolecules and to decorate their surfaces with targeting groups [21] open the possibility to produce in the near future multi-functional vesicles for theranostic applications.

Supporting Information

Supporting Information is available from the Wiley Online Library or from the author.

Acknowledgements
This work was financially supported by MINECO/FEDER, Spain, Grants CTQ2013-40480-R, SAF2016-7524-R, and MAT 2016-80826-R, by AGAUR, Generalitat de Catalunya, Grant 2014-SGR-17 and through the CERCA program, the Networking Research Center on Bioengineering, Biomaterials, and Nanomedicine (CIBER-BBN) and the Spanish Ministry of Economy and Competitiveness, through the "Severo Ochoa" Programme for Centres of Excellence in R & D (SEV-2015-0496, Grant FLOWERS, and SEV-2014-0425). L. A. thanks the financial support of AXA Research Fund and D. H. and E. VS. the Army Research Laboratory, Grant W911NF-15-2-0090. The research leading to these results received funding from the People Programme (Marie Curie Actions) of the European Union's Seventh Framework Programme FP7/2007–2013 under REA grant agreement no. 607721 (Nano2Fun) A. A. and S. I. are enrolled in the Materials Science Ph.D. program of UAB. A. A and S. A. gratefully acknowledge help of Dr. M. Masino in photostability measurements.

Received: ((will be filled in by the editorial staff))
Revised: ((will be filled in by the editorial staff))
Published online: ((will be filled in by the editorial staff))

References

[1] U. Resch-Genger, M. Grabolle, S. Cavaliere-Jaricot, R. Nitschke, T. Nann, *Nat. Methods* **2008**, *5*, 763.

[2] J. W. Lichtman, J.-A. Conchello, *Nat. Methods* **2005**, *2*, 910.

[3] S. Luo, E. Zhang, Y. Su, T. Cheng, C. Shi, *Biomaterials* **2011**, *32*, 7127.

[4] Q. Li, L. Liu, J. W. Liu, J. H. Jiang, R. Q. Yu, X. Chu, *TrAC - Trends Anal. Chem.* **2014**, *58*, 130.

[5] J. Zhang, R. Chen, Z. Zhu, C. Adachi, X. Zhang, C.-S. Lee, *ACS Appl. Mater. Interfaces* **2015**, acsami.5b08539.

[6] J. Mérian, J. Gravier, F. Navarro, I. Texier, *Molecules* **2012**, *17*, 5564.

[7] J. Schill, A. P. H. J. Schenning, L. Brunsveld, *Macromol. Rapid Commun.* **2015**, n/a.

[8] A. Reisch, A. S. Klymchenko, *Small* **2016**, *12*, 1968.

[9] V. Parthasarathy, S. Fery-Forgues, E. Campioli, G. Recher, F. Terenziani, M. Blanchard-Desce, *Small* **2011**, *7*, 3219.

[10] J. U. Menon, P. Jadeja, P. Tambe, K. Vu, B. Yuan, K. T. Nguyen, *Theranostics* **2013**, *3*, 152.

[11] L. Sercombe, T. Veerati, F. Moheimani, S. Y. Wu, A. K. Sood, S. Hua, *Front. Pharmacol.* **2015**, *6*, 1.

[12] S. Li, B. Goins, L. Zhang, A. Bao, *Bioconjug. Chem.* **2012**, *23*, 1322.

[13] V. P. Torchilin, *Nat. Rev. Drug Discov.* **2005**, *4*, 145.

[14] E. M. Agency, **2013**, *44*, 1.

[15] X. Wang, E. J. Danoff, N. a. Sinkov, J. H. Lee, S. R. Raghavao, D. S. English, *Langmuir* **2006**, *22*, 6461.

[16] M. Toprak, B. Meryem Aydn, M. Ark, Y. Onganer, *J. Lumin.* **2011**, *131*, 2286.

[17] V. Deissler, R. Rüger, W. Frank, A. Fahr, W. A. Kaiser, I. Hilger, *Small* **2008**, *4*, 1240.

[18] N. Grimaldi, F. Andrade, N. Segovia, L. Ferrer-Tasies, S. Sala, J. Veciana, N. Ventosa, *Chem. Soc. Rev.* **2016**, *45*, 6520.

[19] L. Ferrer-Tasies, E. Moreno-Calvo, M. Cano-Sarabia, M. Aguilella-Arzo, A. Angelova, S. Lesieur, S. Ricart, J. Faraudo, N. Ventosa, J. Veciana, *Langmuir* **2013**, *29*, 6519.

[20] E. Elizondo, J. Larsen, N. S. Hatzakis, I. Cabrera, T. Bjørnholm, J. Veciana, D. Stamou, N. Ventosa, *J. Am. Chem. Soc.* **2012**, *134*, 1918.

[21] I. Cabrera, E. Elizondo, O. Esteban, J. L. Corchero, M. Melgarejo, D. Pulido, A. Córdoba, E. Moreno, U. Unzueta, E. Vazquez, I. Abasolo, S. Schwartz, A. Villaverde, F. Albericio, M. Royo, M. F. García-Parajo, N. Ventosa, J. Veciana, *Nano Lett.* **2013**, *13*, 3766.

[22] E. Elizondo, J. Veciana, N. Ventosa, *Nanomedicine* **2012**, *7*, 1391.

[23] I. Texier, M. Goutayer, A. Da Silva, L. Guyon, N. Djaker, V. Josserand, E. Neumann, J. Bibette, F. Vinet, *J. Biomed. Opt.* **2015**, *14*, 54005.

[24] A. Wagh, S. Y. Qian, B. Law, *Bioconjug. Chem.* **2012**, *23*, 981.

[25] X. Zhuang, *Nat Phot.* **2009**, *3*, 365.

[26] A. M. Vinogradov, A. S. Tatikolovab, S. M. B. Costa, **2001**.

[27] D. a. K. B. J.S. Dua, Prof. A. C. Rana, *Int. J. Pharm. Stud. Res.* **2012**, *3*, 7.

[28] S. Gadde, E. K. Batchelor, A. E. Kaifer, *Chem. - A Eur. J.* **2009**, *15*, 6025.

[29] A. Mishra, R. K. Behera, P. K. Behera, B. K. Mishra, G. B. Behera, *Chem. Rev.* **2000**, *100*, 1973.

[30] G. B. Behera, P. K. Behera, B. K. Mishra, *J. Surf. Sci. Technol.* **2007**, *23*, 1.

[31] Y. Kawabe, S. Kato, *Dye. Pigment.* **2012**, *95*, 614.

[32] C. C. Corredor, K. D. Belfield, M. V Bondar, O. V Przhonska, S. Yao, *J. Photochem. Photobiol. A Chem.* **2006**, *184*, 105.

[33] H.-Y. Ahn, S. Yao, X. Wang, K. D. Belfield, *ACS Appl. Mater. Interfaces* **2012**, *4*, 2847.

[34] G. V Zakharova, A. K. Chibisov, **2009**, *43*, 346.

[35] M. M. S. Abdel-mottaleb, M. Van Der Auweraer, M. S. A. Abdel-mottaleb, **2004**, *6*, 2.

[36] J. Fu, L. a. Padilha, D. J. Hagan, E. W. Van Stryland, O. V. Przhonska, M. V. Bondar, Y. L. Slominsky, A. D. Kachkovski, *J. Opt. Soc. Am. B* **2007**, *24*, 56.

[37] J. C. Phillips, R. Braun, W. Wang, J. Gumbart, E. Tajkhorshid, E. Villa, C. Chipot, R. D. Skeel, L. Kalé, K. Schulten, *J. Comput. Chem.* **2005**, *26*, 1781.

[38] P. F. F. Al. and W. L. . Vaz, in *Handb. Biol. Phys.*, Elsevier Science, Amsterdam, 1995, **1995**, pp. 367–373.

[39] D. Van Der Zwaag, N. Vanparijs, S. Wijnands, R. De Rycke, B. G. De Geest, L. Albertazzi, *ACS Appl. Mater. Interfaces* **2016**, *8*, 6391.

[40] L. Albertazzi, R. W. Van Der Hofstad, E. W. Meijer, *Science* **2014**, *491*, 10.

[41] W. Humphrey, A. Dalke, K. Schulten, *J. Mol. Graph.* **1996**, *14*, 27.

[42] T. Giorgino, *Comput. Phys. Commun.* **2014**, *185*, 317.

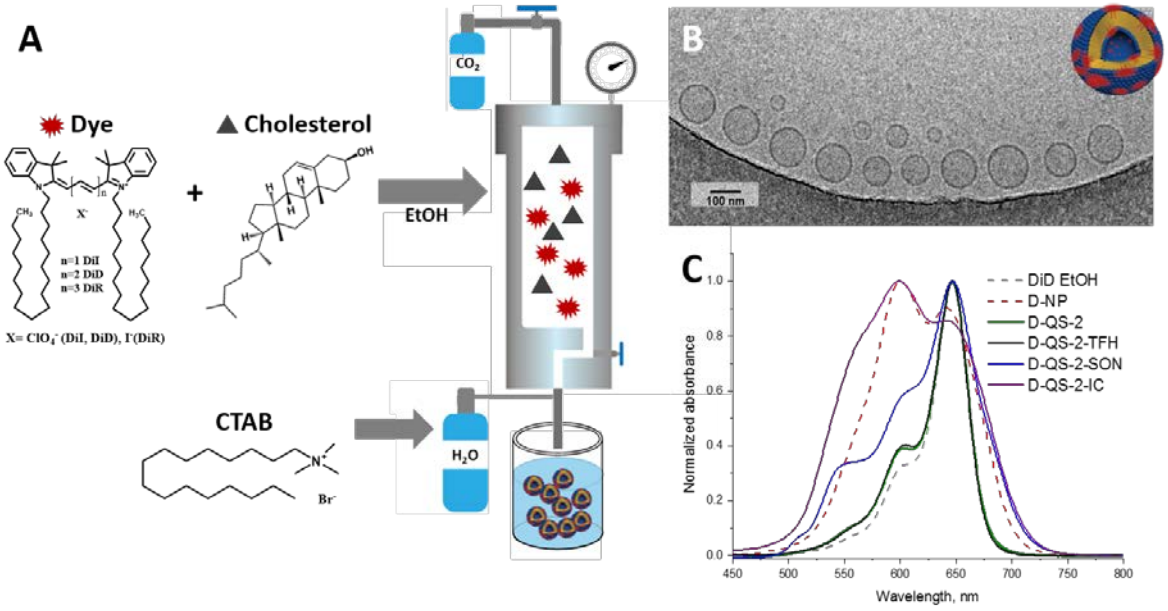

Figure 1. A) Schematic representation of DELOS-SUSP method for the preparation of Quatsomes loaded with dyes (DiI, DiD and DiR). B) CryoTEM image of D-QS-2 and C) absorption spectra of DiD in EtOH, DiD-based NPs and D-QS prepared by different methods (see Text).

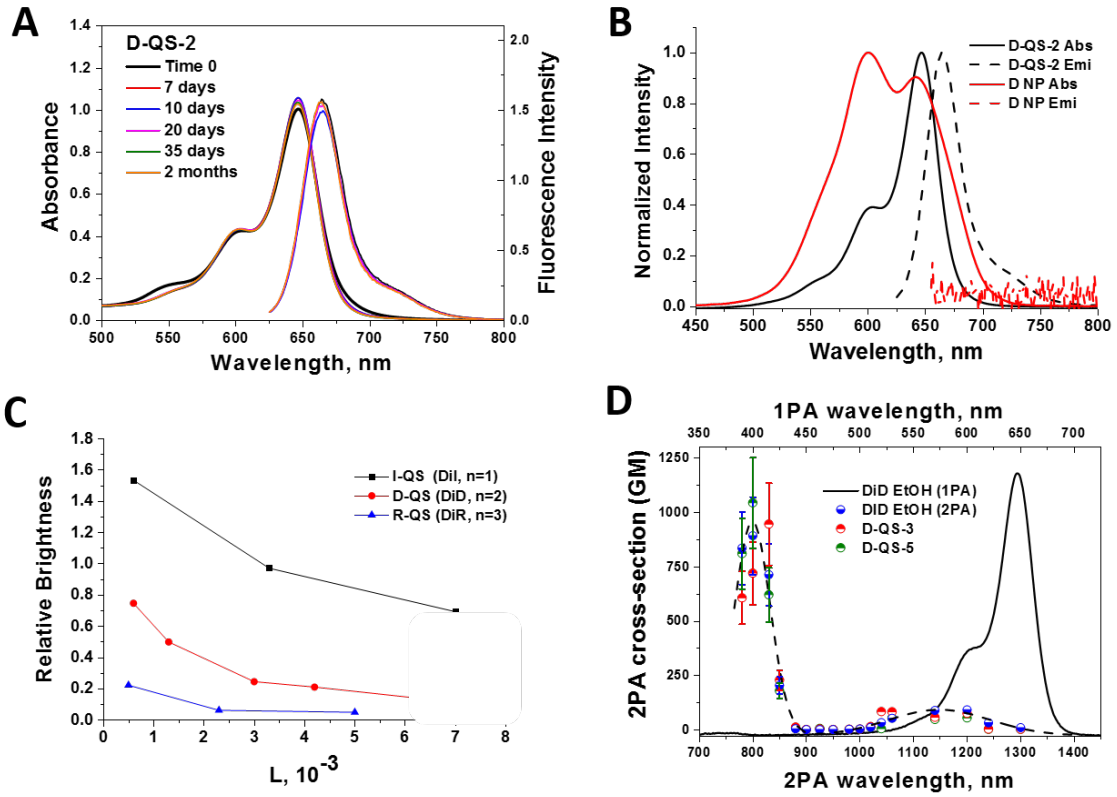

Figure 2. a) Stability of D-QS-2 sample in water evaluated by UV-vis absorption and emission spectra (λ_{exc} = 610 nm) monitored over two months b) Normalized UV-vis absorption and emission of D-QS-2 and D-NP; c) Relative brightness ($Brightness_{sample}/Brightness_{dye(EtOH)}$) vs loading of the different cyanines-loaded QSs; d) One- (solid line) and two-photon (blue circles) spectra of DiD in EtOH and two-photon spectra of D-QS-3 (red-circles) and D-QS-5 (green circles). The dashed line with the shape of the 2PA spectra is shown as guide to the eye.

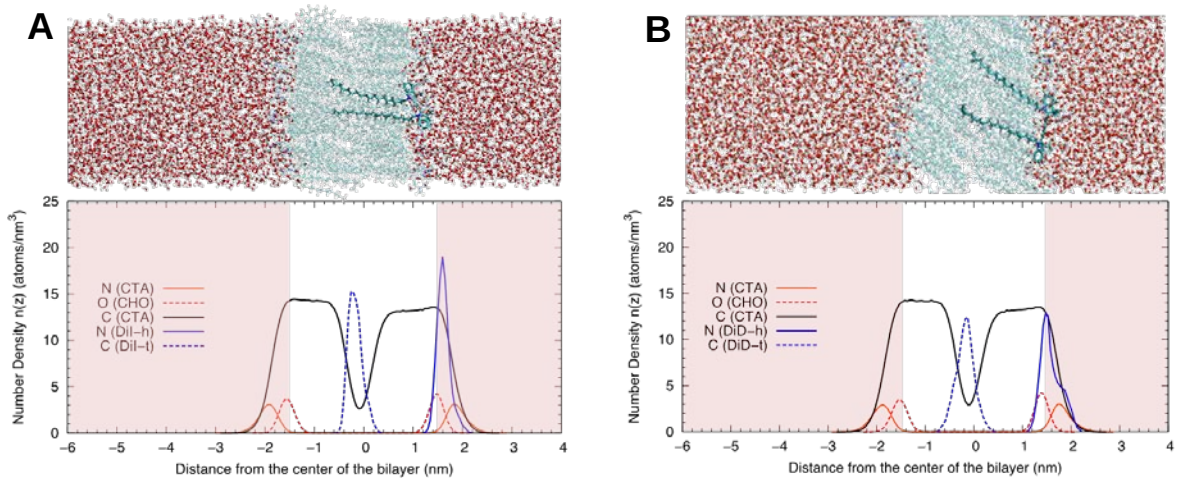

Figure 3. Results from MD simulations for hydrophobic dyes in QSss: (A) DiI and (B) DiD. For each dye, we show a representative snapshot and the average atomic density profiles of selected atoms in the direction perpendicular to the QS bilayer. In the snapshots, CTAB molecules, water molecules and the dye molecule (emphasized) are shown in CPK representation. Cholesterol molecules and ions are not shown for clarity. The atomic density profiles indicate the location of two characteristic dye atoms (N from the carbocyanines and terminal C from the alkyl chain), the location of the hydrophobic core (C atoms from CTAB) and the hydrophilic headgroup region (defined by oxygen atoms from cholesterol –OH and nitrogen atoms from CTAB). The atomic density for dye atoms is multiplied by 100 to help identification of the peaks. The region occupied with water is indicated with a shadow to help interpretation of atomic density profiles. The snapshots and density profiles were made using VMD[41,42].

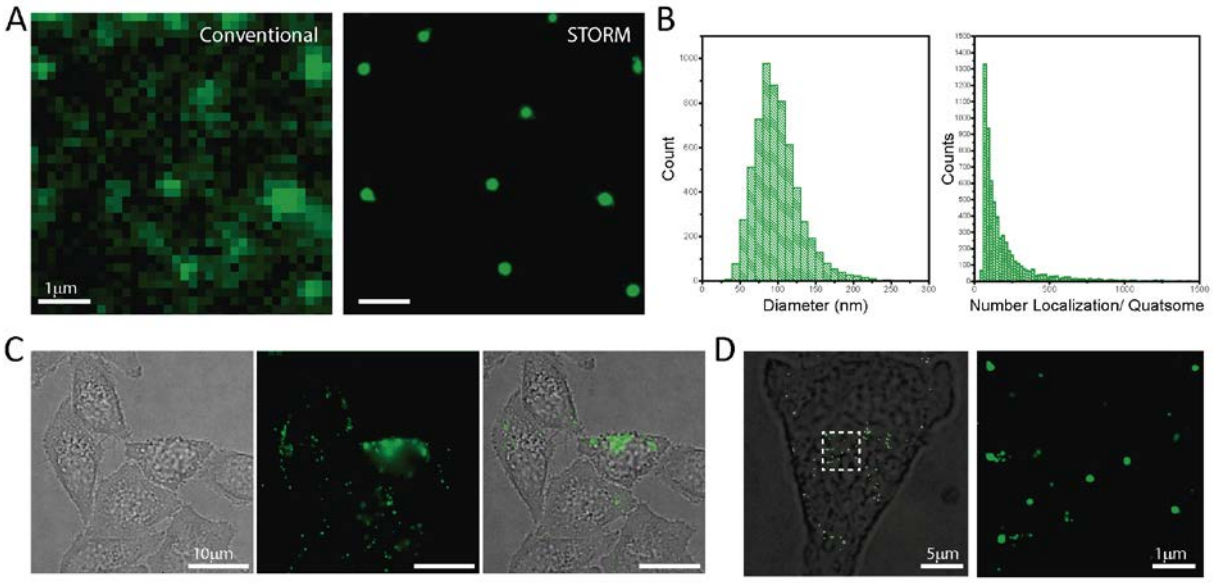

Figure 4. A) Images of DiI-loaded Quatsomes (I-QS-1) obtained by conventional wide-field microscopy and STORM (λ_{exc} = 561 nm). B) Distribution of size and number of localizations per Quatsomes extrapolated from STORM images. C) Snapshot of the video (see SI) acquired by fluorescence microscopy of the internalization of QSs in HeLa cells. D) STORM images of QSs internalized in HeLa cells.

Nanostructuring lipophilic dyes in water using stable vesicles, Quatsomes, leads to a new class of fluorescent nanoparticles with superior stability and structural homogeneity. The new probes show enhanced optical properties (i.e. brightness) when compared to other nanoparticles and are suitable for application in super-resolution microscopy techniques (STORM). Fluorescent Quatsomes constitute a promising nanomaterial for imaging and theranostics applications.

Keywords: Vesicles, dyes, fluorescent nanoparticles, Molecular Dynamics, STORM

A. Ardizzone, S. Kurhuzenkau, S. Illa, J. Faraudo, M. Bondar, D.J. Hagan, E.W. Van Stryland, A. Painelli, C. Sissa, N. Feiner, L. Albertazzi, J. Veciana*, N. Ventosa*

Nanostructuring Lipophilic Dyes in Water Using Stable Vesicles – Quatsomes – as Scaffolds and their use as Probes for Bioimaging

ToC figure (55mm x 50 mm)